

# Zirconium Hydroxide–Metal–Organic Framework Composites for Toxic Chemical Removal

Gregory W. Peterson,<sup>\*,†</sup> Joseph A. Rossin,<sup>§</sup> Jared B. DeCoste,<sup>⊥</sup> Kato L. Killops,<sup>†</sup> Matthew Browe,<sup>†</sup> Erica Valdes,<sup>†</sup> and Paulette Jones<sup>⊥</sup>

<sup>†</sup>Edgewood Chemical Biological Center, 5183 Blackhawk Road, APG, Maryland 21010-5424, United States

<sup>§</sup>Guild Associates, Inc., 5750 Shier Rings Road, Dublin, Ohio 43016, United States

<sup>⊥</sup>SAIC, Inc., P.O. Box 68, Gunpowder, Maryland 21010-0068, United States

## S Supporting Information

**ABSTRACT:** Composite materials comprising the metal–organic framework CuBTC (HKUST-1 or  $\text{Cu}_3(\text{BTC})_2$ ) and zirconium hydroxide were made to develop a material capable of broad spectrum toxic chemical removal. Materials were physically mixed at varying percentages, followed by pressing into pellets to set the structure. Mixtures were confirmed using powder X-ray diffraction, attenuated total reflectance–Fourier transform infrared spectroscopy, X-ray photoelectron spectroscopy, and scanning electron microscopy. Nitrogen isotherm data were collected on the composite media, followed by breakthrough testing against ammonia, cyanogen chloride, and sulfur dioxide. All samples exhibited substantial porosity. As the percentage of CuBTC increased, ammonia performance increased while sulfur dioxide removal generally decreased. Cyanogen chloride removal increased with increased CuBTC percentage under dry conditions, but failed to provide any significant removal under humid conditions. Adding triethylenediamine to the composites resulted in a substantial increase in cyanogen chloride removal capacity under humid conditions. In all, the composite structures resulted in some synergistic effects for ammonia and cyanogen chloride, with removal capacities higher than weighted averages based on performance of pure components. Data indicate that composites comprising CuBTC and zirconium hydroxide may be viable for broad spectrum toxic chemical filtration.

## 1. INTRODUCTION

As the chemical industry continues to grow, the filtration of toxic chemicals is a major focus in current sorbent development. Efforts are ongoing to develop materials capable of high capacity removal of specific chemicals, such as hydrogen cyanide,<sup>1</sup> ammonia,<sup>2</sup> cyanogen chloride,<sup>3</sup> arsine,<sup>4,5</sup> hydrogen sulfide,<sup>6</sup> methyl bromide,<sup>7</sup> and others. Indeed, many of these materials provide substantial removal capabilities; however, many of the efforts focus on optimization against a single toxic gas. In particular, materials capable of broad spectrum protection, to include acidic and basic gases in support of military and National Institute for Occupational Safety and Health (NIOSH) Chemical Biological Radiological and Nuclear (CBRN) filtration devices are sought.<sup>8,9</sup>

The removal of acidic and basic gases on a single filtration media creates a unique challenge to developers of filtration media. This is because acidic gases, such as chlorine, phosgene, and sulfur dioxide, are removed via reactions with basic sites. Conversely, basic gases, such as ammonia, are removed by reactions involving acidic sites. Acidic and basic sites on a single surface have the potential to interact and neutralize one another, especially when the sites are not properly segregated. As such, an approach must be taken to either anchor sorbent functional groups to the substrate, or physically separate the dissimilar functionalities such that deleterious effects do not occur.

A variety of noncarbon materials have been in development over the past several years targeting toxic gas removal. Britt and co-workers first demonstrated the use of metal–organic

frameworks (MOFs) to remove a variety of toxic chemicals,<sup>10</sup> and Peterson et al. further demonstrated the applicability of MOFs for these applications.<sup>11</sup> In particular, Peterson and co-workers found that the MOF CuBTC (HKUST-1 or  $\text{Cu}_3(\text{BTC})_2$ )<sup>12</sup> provided efficient ammonia removal<sup>13</sup> and can furthermore be stabilized to reduce aging.<sup>14</sup>

Previous studies have shown that zirconium hydroxide is an effective material for the removal of a wide range of toxic chemicals, especially acidic/acid-forming gases, including cyanogen chloride,<sup>15</sup> chlorine, phosgene, hydrogen chloride,<sup>16</sup> and sulfur dioxide.<sup>17,18</sup> Furthermore, zirconium hydroxide is known to provide reactive removal of chemical warfare agents such as O-ethyl S-[2-(diisopropylamino)ethyl] methylphosphonothioate (VX) and O-pinacolyl methylphosphonofluoride (GD, or Soman).<sup>19</sup> Zirconium hydroxide, due to its basic nature, is not expected to provide adequate removal capabilities against basic chemicals.

Together, CuBTC and zirconium hydroxide may provide a composite capable of broad spectrum chemical removal. Composite structures including MOFs have been previously investigated for a variety of applications, including toxic chemical removal. Metal–organic frameworks have been templated with metal oxides such as iron oxide,  $\text{Fe}_2\text{O}_3$ , and titania,  $\text{TiO}_2$ , for hydrogen production.<sup>20</sup> Jahan and co-workers

Received: January 30, 2013

Revised: March 17, 2013

Accepted: March 18, 2013

Published: March 18, 2013

grew porphyrin-MOFs from graphene building blocks for use in redox chemistry.<sup>21</sup> O'Neill and co-workers investigated a physical mixture of polyacrylamide (PAM) with CuBTC and CPO-27 (aka MOF-74), and characterized the material for nitrogen adsorption and mechanical properties.<sup>22</sup> Bandosz and colleagues investigated the CuBTC/graphite oxide (GO) system for use as an ammonia sorbent,<sup>23</sup> and Bandosz and Petit developed several additional MOF/GO composites.<sup>24</sup> This latter effort in particular is intriguing, as several materials were evaluated against ammonia, hydrogen sulfide, and nitrogen dioxide, showing high loadings for several materials.

The objective of this paper is to develop and evaluate materials capable of achieving broad spectrum chemical protection. To meet this objective, physical mixtures of the zirconium hydroxide and CuBTC at varying loadings were prepared, with zirconium hydroxide targeting acidic/acid-forming gases and CuBTC targeting ammonia. Characterization of the composites is carried out using a variety of techniques, while performance characteristics of the composites are determined using breakthrough techniques.

## 2. EXPERIMENTAL SECTION

Zirconium hydroxide was received from MEL Chemicals (Flemington, NJ) and CuBTC MOF was purchased from Sigma Aldrich. Materials were physically mixed by shaking the desired ratio of CuBTC and zirconium hydroxide for approximately 1 min. The powders were intimately mixed by shaking for approximately 1 min, and then pelletized using a Carver press at 5000 psi for 1 min such that the composite was set. The composite structure was then crushed using a mortar and pestle into a powder and forwarded for characterization and breakthrough testing. The materials are notated as pure zirconium hydroxide (100Z), a physical mixture of 90 wt% zirconium hydroxide, 10 wt% CuBTC (90Z/10C), 75 wt% zirconium hydroxide, 25 wt% CuBTC (75Z/25C), 50 wt% zirconium hydroxide + 50 wt% CuBTC (50Z/50C), and pure CuBTC (100C). Each composite sample was also loaded with triethylenediamine (TEDA or DABCO, Sigma Aldrich) to 5 wt % (nominal) to produce 90Z/10C-ST, 75Z/25C-ST, and 50Z/50C-ST, respectively. TEDA was sublimed onto the samples in an oven at 60 °C for approximately 24 h while rotating to provide an even distribution. The weight percentage was based on the mass of the individual components.

X-ray diffraction patterns were measured with a Philips diffractometer equipped with an XCelerator detector using CuK $\alpha$  radiation, a spinning sample stage, and a scan range of 10–80 2 $\theta$ .

Attenuated total reflectance-Fourier transform infrared (ATR-FTIR) spectroscopy data were collected on composites using a Bruker Tensor 27 FTIR with a platinum accessory and a single reflection diamond crystal. The 16 scans from 4000 to 600 cm $^{-1}$  were averaged, and the background was subtracted with a resolution of 4 cm $^{-1}$ .

X-ray photoelectron spectroscopy (XPS) spectra were recorded using a Perkin-Elmer Phi 570 ESCA/SAM system employing MgK $\alpha$  X-rays. For the physical mixtures, the charging of the two dissimilar components of mixture differed, with the zirconium hydroxide charging more than the MOF. As a result, elements associated with the zirconium hydroxide were referenced to the Zr 2p3/2 photoelectron peak at 182.1 eV, while elements associated with the MOF were referenced to the C1s photoelectron peak at 284.6 eV.

Images of the composites were obtained with a JEOL 7001 scanning electron microscope (SEM) with field emission and low vacuum capabilities. An Oxford energy dispersive spectroscopy (EDS) equipped with an 80 mm $^2$  X-Max detector and INCA software was used to map zirconium and copper on the composites.

Nitrogen isotherm data were collected at 77 K using a Micromeritics ASAP1200 system. Samples were off-gassed at 90 °C for approximately 12–24 h until a pressure of less than 10 millitorr was achieved and maintained for 30 min. Surface area measurements were calculated using the Brunauer–Emmett–Teller (BET) method and pore volume was calculated at a relative pressure of 0.975.

Breakthrough testing was conducted on a push system designed for evaluating small (mg) quantities of powders, and has been described previously.<sup>11,13</sup> Test conditions are summarized in Table 1. Briefly, sorbents were activated at 80

**Table 1. Breakthrough Parameters**

parameter	value
temperature	20 °C
RH	0% (−40 °C dew point), 80% RH
adsorbent mass	~15–40 mg
adsorbent volume	55 mm $^3$
flow rate	20 mL/min
challenge concentration	1000 mg/m $^3$ (ammonia, sulfur dioxide) 4000 mg/m $^3$ (cyanogen chloride)

°C for 1 h in flowing bone-dry air, equilibrated at the proper relative humidity (RH) for 2 h, and then packed at a constant volume of approximately 55 mm $^3$  in a 4 mm inside diameter (nominal) fritted glass tube to a height of 4 mm. For ammonia, cyanogen chloride (CNCl), and sulfur dioxide, chemicals were injected into a ballast and then pressurized. For all chemicals, the chemical was delivered to a dry or humidified stream at rates necessary to achieve the challenge concentrations as summarized in Table 1. Humidity was delivered to the system via saturator cells within a water bath. The challenge was dosed to the packed beds until saturation (effluent = feed) occurred, after which air was purged to the materials to evaluate desorption. Effluent concentrations were monitored using Hewlett-Packard gas chromatographs equipped with a flame ionization detector (CNCl), a photoionization detector (ammonia), and a flame photometric detector (sulfur dioxide).

Breakthrough graphs are plotted on a mass-weighted basis to account for differences in density. Loadings were calculated in mol/kg by integrating the breakthrough curves to saturation. The standard system error is approximately 10%. Hypothetical loadings were determined by taking a weighted average of the pure Zr(OH) $_4$  and CuBTC loadings for each chemical.

## 3. RESULTS AND DISCUSSION

**3.1. Materials Characterization.** Figure 1 illustrates the PXRD patterns and ATR spectra for the pure and composite materials. The pure zirconium hydroxide material, 100Z, is mostly amorphous to X-ray, and only shows broad peaks around 2 theta values of 25 and 50. The 90Z/10C sample does not show the presence of CuBTC in the X-ray pattern, likely due to interference or noise from the zirconium amorphous pattern; however, the ATR spectrum does indeed show the presence of CuBTC. The other composites show the presence of both zirconium hydroxide and CuBTC. Only data under

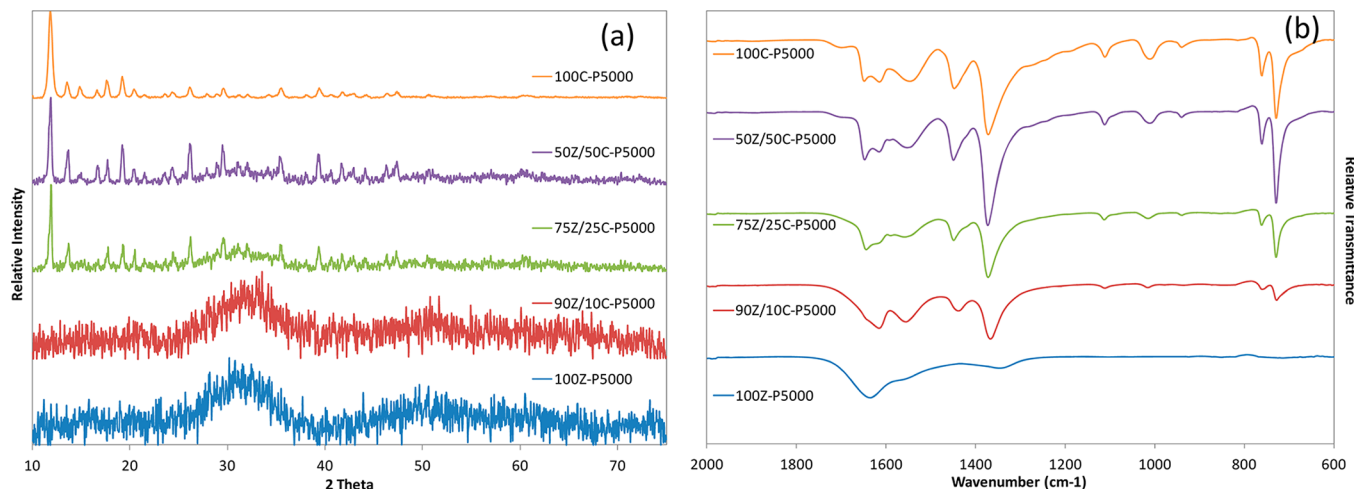


**Figure 1.** PXRD (a) and ATR-FTIR (b) spectra of composite materials. Both analyses indicate that CuBTC structure remains intact in the composite materials.

**Table 2. XPS Data for Composite Samples<sup>a</sup>**

sample	Cu/Zr (At)	CuBTC/Zr(OH) <sub>4</sub> (wt)
100Z	n/a	n/a
90Z/10C	0.10	0.12
75Z/25C	0.20	0.25
50Z/50C	0.42	0.53
100C	n/a	n/a

<sup>a</sup>The Cu/Zr ratios indicate that the composites correspond well to the percentages used for physically mixing the components.

2000 cm<sup>-1</sup> are shown in the Figure 1b, as data above that are convoluted with bulk water (shown in Figure S1 in the Supporting Information). Peak values have been previously assigned by others for Zr(OH)<sub>4</sub><sup>18</sup> and CuBTC;<sup>25</sup> in Figure 1b, it is clear that as the percentage of CuBTC increases, the peaks associated with the MOF sharpen and increase in intensity, indicating a good mixture of the individual components.

XPS data were collected to determine if the distribution within the composites was commensurate with the starting mixture. Table 2 summarizes the results. Of particular note is the Cu/Zr atomic ratios, which were corrected to weight ratios of CuBTC to Zr(OH)<sub>4</sub> based on the molecular weights of the materials. The 90Z/10C sample shows approximately 12% CuBTC, slightly higher than the targeted value, the 75Z/25C exhibits exactly 25% CuBTC, and the 50Z/50C samples exhibits 47% CuBTC, slightly lower than the targeted value. In

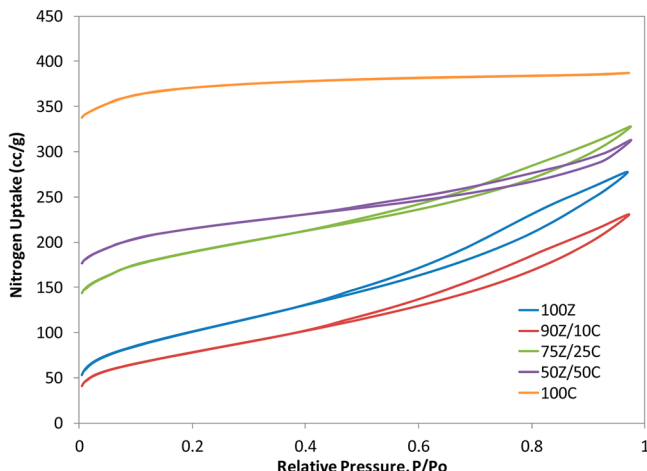


**Figure 3.** Nitrogen adsorption and desorption isotherms for pure component and composite materials. Data correspond to media following preparation into particles.

any case, the ratios are in relatively good agreement with the expected percentages. One interesting note is that the copper present in the 90Z/10C composite was Cu(I), yet in the other samples was present as Cu(II), indicating possible degradation of the sample.

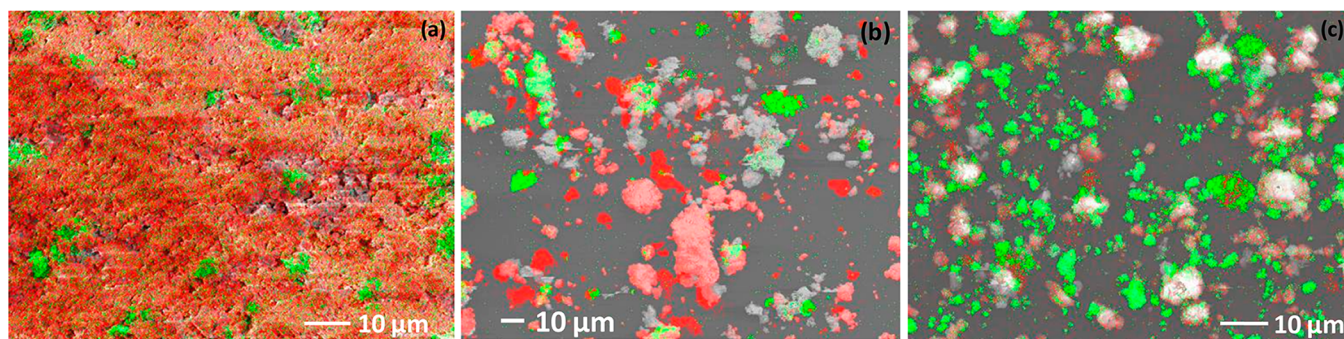


**Figure 2.** SEM images with overlaid X-ray maps (a) 90Z/10C, (b) 75Z/25C, and (c) 50Z/50C composites. Copper presents as green, while zirconium presents in red. The distributions are consistent with the physical mixture percentages as well as the XPS results.

**Table 3. Summary of Physical Properties for Pure Component and Composite Materials**

sample	packing density (g/cc)	surface area		pore volume	
		(m <sup>2</sup> /g)	(m <sup>2</sup> /cc)	(cc/g)	(cc/cc)
100Z	0.59	359	211	0.43	0.25
90Z/10C	0.57	278	158	0.36	0.20
75Z/25C	0.54	691	371	0.51	0.27
50Z/50C	0.49	806	391	0.48	0.23
100C	0.43	1462	624	0.60	0.26

SEM images and X-ray maps were taken to further illustrate the distribution of copper and zirconium in the composites, and are shown in Figure 2. Note that, as the percentage of CuBTC increases, the amount of copper, presented as green maps overlaid on the SEM images increases, further indicating a good physical mixture of components.

Nitrogen isotherm data were collected for all samples and are shown in Figure 3. Surface area and pore volume results are summarized in Table 3. Both surface area and pore volume are also reported on a volume basis, as the metal oxide and MOF have very different densities, as shown in Table 2. The pure CuBTC material provides the highest nitrogen uptake as well as

**Table 4. Ammonia Saturation Loadings of Materials**

sample	loading (mol/kg)	
	dry	humid
100Z	0.9	0.5
90Z/10C	1.4	1.5
75Z/25C	2.4	5.2
50Z/50C	4.4	5.8
100C	7.8	7.7

the highest surface area. In general, as CuBTC percentage decreases, the surface area and porosity also decrease. The one exception exists with the 90Z/10C sample as compared to the pure Zr(OH)<sub>4</sub> material; the former shows slightly lower nitrogen uptake and surface area as compared to the pure component. Multiple possible explanations exist for this behavior. First, it is possible that, during pressing, some of the more porous CuBTC component was blocked off, or encapsulated, by the much higher weight percentage of zirconium, resulting in lower nitrogen uptake. Another explanation is that the CuBTC component was degraded due to the presence of excessive moisture in the zirconium hydroxide component, and lost porosity before nitrogen

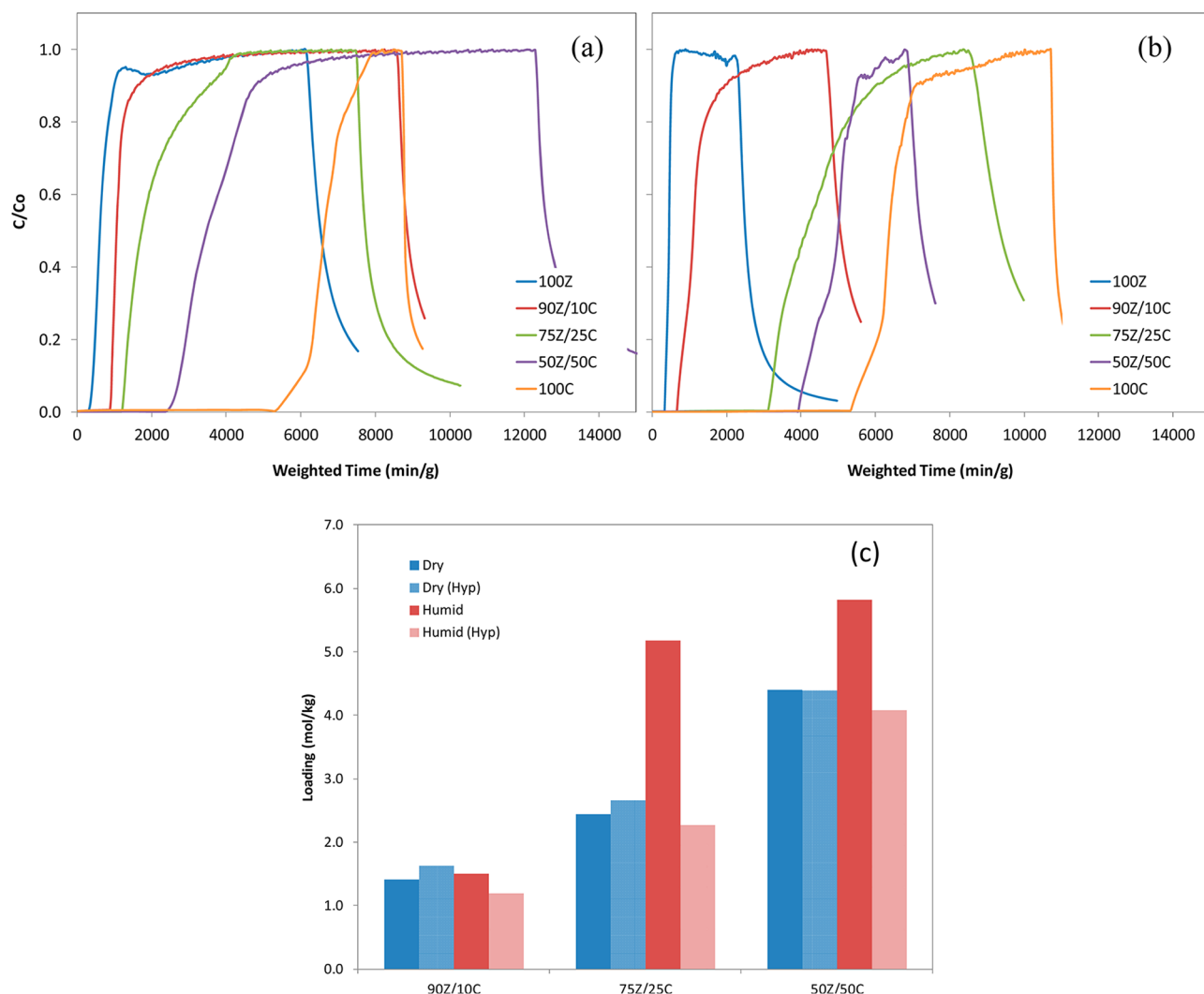


**Figure 4.** Ammonia breakthrough of composites under (a) dry and (b) humid conditions. Composite structure performance is shown in panel c and indicates there are synergistic effects due to mixing the materials.

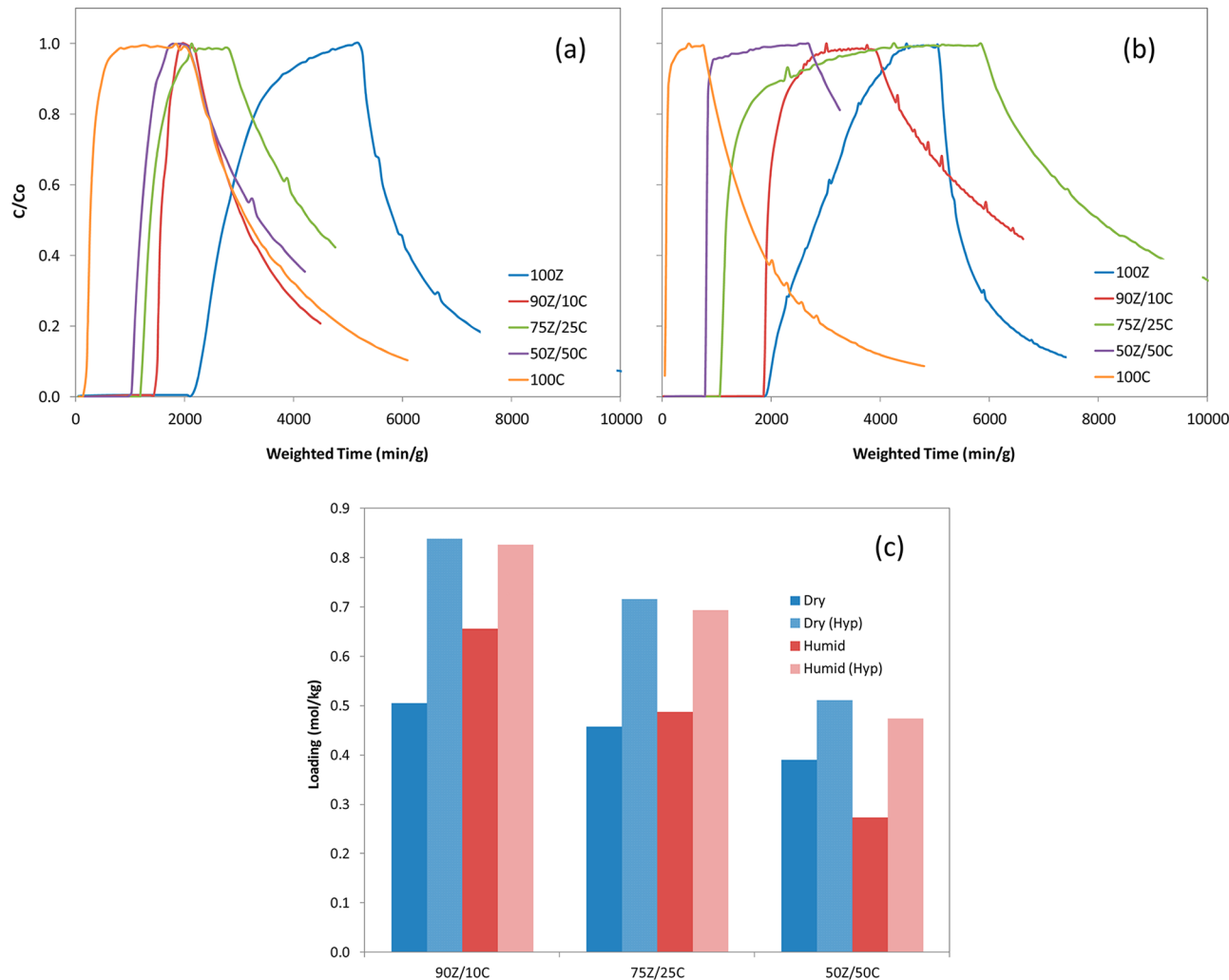


**Figure 5.** Sulfur dioxide breakthrough of composites under (a) dry and (b) humid conditions. Composite structure performance is shown in panel c and indicates there is no synergy by mixing the materials.

**Table 5. Sulfur Dioxide Saturation Loading of Materials**

sample	loading (mol/kg)	
	dry	humid
100Z	0.9	0.9
90Z/10C	0.5	0.7
75Z/25C	0.5	0.5
50Z/50C	0.4	0.3
100C	0.1	0.0

porosimetry was conducted. The latter explanation, which is backed up by XPS results, would also be seen with the other components; however, due to the lower weight percentages of CuBTC in the 90Z/10C and 75Z/25C composites, the loss of porosity is not as noticeable. In any case, all samples show significant surface area and porosity. The pure CuBTC material exhibits behavior typical of a microporous material and a Type I isotherm. As zirconium hydroxide content increases, the isotherm transitions to more of a Type II shape. Coupled with hysteresis seen for the composite samples and pure zirconium hydroxide material, this behavior is indicative of the presence of larger mesopores.

**3.2. Chemical Breakthrough.** Materials were evaluated for their ability to remove ammonia, sulfur dioxide, and cyanogen

chloride to evaluate their performance against common industrial chemicals. Figure 4 illustrates the breakthrough curves for ammonia. Under dry conditions, the pure zirconium hydroxide material (100Z) exhibits relatively fast ammonia breakthrough, while the pure CuBTC material (100C) exhibits very slow ammonia breakthrough, indicating a much larger capacity for the CuBTC MOF as compared to the metal hydroxide as expected based on previous studies.<sup>13</sup> The composite materials follow the expected trend, with the 90Z/10C sample providing slightly higher ammonia removal as compared to the pure zirconium hydroxide material, followed by 75Z/25C sample and the 50Z/50C samples, respectively. The calculated loadings, summarized in Table 4, indicate the same trend, and loadings follow the percentage of CuBTC in the material. These loadings are compared to the hypothetical loadings calculated based on a weighted average of the pure components (Figure 4c). For the pure MOF material, a loading of 7.7 mol/kg was calculated, while the pure zirconium hydroxide material exhibits almost 1.0 mol/kg. The loading for the 50Z/50C sample is almost exactly in the middle of the pure components, with a loading of 4.4 mol/kg, and corresponds well to the hypothetical loading. The other two composites, 90Z/10C and 75Z/25C, have ammonia loadings of

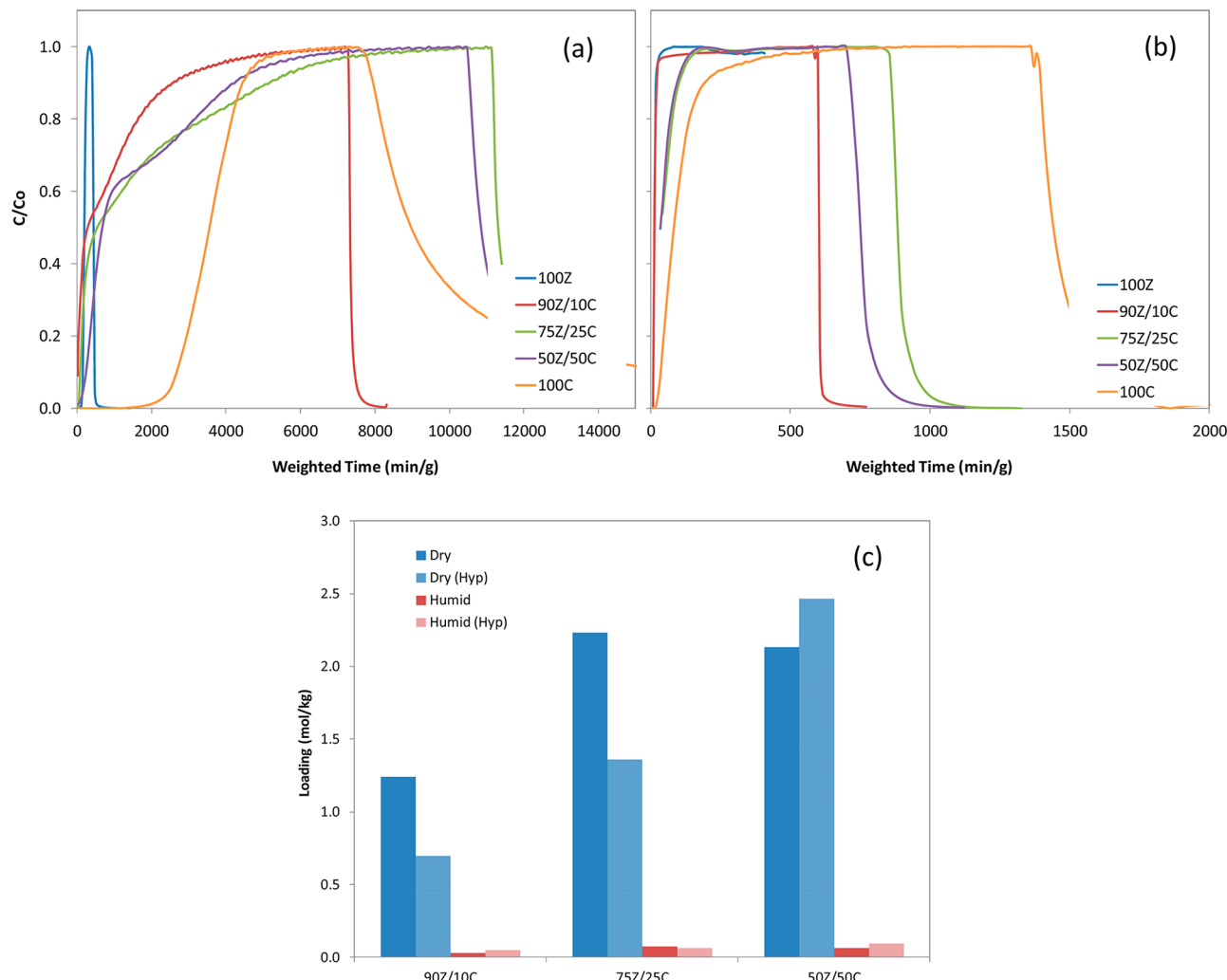


**Figure 6.** Cyanogen chloride breakthrough of composites under (a) dry and (b) humid conditions. Actual as compared to hypothetical loadings are compared in panel c.

**Table 6. CNCI Saturation Loadings of Materials**

sample	loading (mol/kg)	
	dry	humid
100Z	0.3	0.0
90Z/10C	1.2	0.0
75Z/25C	2.2	0.1
50Z/50C	2.1	0.1
100C	4.7	0.1
90Z/10C-ST	1.2	1.9
75Z/25C-ST	0.6	1.4
50Z/50C-ST	1.1	0.6

1.4 and 2.4, respectively, corresponding well with the hypothetical loadings.

Under humid conditions, the pure zirconium hydroxide performance decreases slightly, achieving an ammonia loading of only 0.5 mol/kg, while the pure CuBTC loading remains consistent with that recorded under dry condition (7.7 mol/kg). The decrease in ammonia loading of zirconium hydroxide is likely due to blocking of active sites by moisture coupled with the sheet-like pores of the material, reducing the dwell time within the pore structure. This is not a problem in the CuBTC MOF, as moisture increases solubility within the extended 3-

dimensional pores. The 90Z/10C composite also remains consistent with the dry condition, with a loading of 1.5 mol/kg. Of particular note, however, are the 75Z/25C and 50Z/50C composites. Each of these samples provides improved ammonia removal than that achieved under dry conditions, and both composites perform significantly better than the theoretical loading, indicating synergistic effects of the physical mixture. In particular, the 75Z/25C sample provides almost double the ammonia capacity as compared to the hypothetical loading. This behavior may be due to the preloaded moisture of both materials, especially, zirconium hydroxide, allowing ammonia to enter into solution and therefore react with the CuBTC MOF substrate more efficiently. Under both dry and humid conditions, the desorption curves are relatively sharp, especially as CuBTC percentage increases, indicating strong retention/reaction of ammonia with the composites. Compared to a broad spectrum carbon used in filters from 3M, the composites exhibit similar or greater ammonia removal capacities (Table S1 in Supporting Information).

Sulfur dioxide was challenged to materials at a concentration of 1000 mg/m<sup>3</sup>, and the results are shown in Figure 5. The calculated loadings are summarized in Table 5. Under dry conditions, pure zirconium hydroxide displays the greatest SO<sub>2</sub> removal capacity, while the CuBTC displays almost no SO<sub>2</sub>

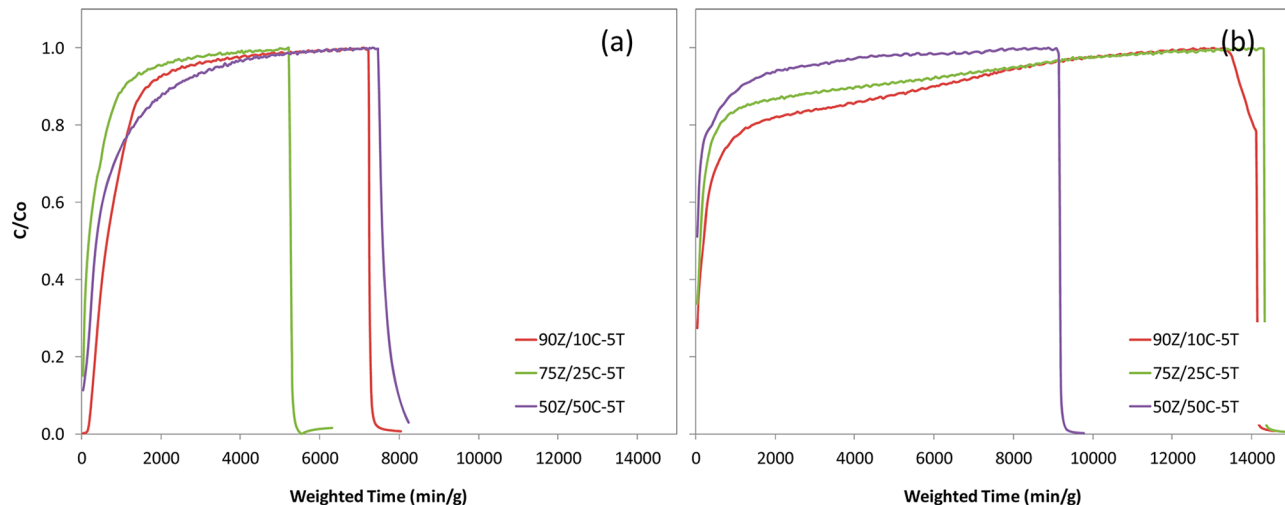


**Figure 7.** Cyanogen chloride breakthrough of composites loaded with TEDA under (a) dry and (b) humid conditions.

removal capability. This is expected, as zirconium hydroxide is known to provide substantial sulfur dioxide removal capabilities,<sup>17</sup> whereas CuBTC has no available SO<sub>2</sub> removal mechanism, thus the poor performance. As with the ammonia results, breakthrough curves correspond well to the percentage of CuBTC, although with an opposite effect. As CuBTC percentage increases, sulfur dioxide removal decreases. Sulfur dioxide removal under humid conditions follows a similar trend, with pure zirconium hydroxide performing the best, and composites showing decreasing performance with decreasing zirconium hydroxide content. Compared to the dry conditions, similar performance is achieved for the pure components as well as the composites, to within experimental error. Compared to the pure components, clearly having a physical mixture is detrimental to the overall capacity, as the composites exhibit decreased capacity much more than the percentage decrease in zirconium hydroxide. This is seen through the calculated loadings as compared to the hypothetical loadings, in which the former are significantly lower than the latter. Therefore, there is no synergy for sulfur dioxide removal by physically mixing these materials. The composite materials exhibit better removal under low RH conditions, but slightly lower sulfur dioxide removal under humid conditions, as compared to the 3M broad spectrum carbon.

Cyanogen chloride breakthrough results are illustrated in Figure 6, and loadings are summarized in Table 6. Under dry conditions, CuBTC exhibits a high capacity for CNCl, with a loading of 4.7 mol/kg. The removal of CNCl is likely due to an interaction with the unsaturated copper centers within the MOF. On the other hand, zirconium hydroxide provides almost no removal by itself; however, with the incorporation of CuBTC into the composites, a relatively high loading is achieved. For all composites, breakthrough occurs quite rapidly; however, it takes a relatively long time to reach saturation, indicating that, although zirconium hydroxide by itself has limited CNCl removal capacity, incorporating CuBTC results in some removal capabilities. As compared to the hypothetical loadings, the composites show strong synergistic effects. Under humid conditions, all show almost immediate CNCl breakthrough to saturation, indicating that moisture sufficiently poisons any sorption sites capable of chemical removal. It is not unexpected that CNCl breaks through almost immediately

under humid conditions, as it is known that the chemical requires catalysts to promote hydrolysis.<sup>3</sup>

As such, TEDA was added to the composites to determine if they could provide enhanced CNCl removal. Figure 7 illustrates the breakthrough curves for the TEDA-loaded samples. Under dry conditions, in general TEDA seems to decrease the CNCl removal capabilities, likely because it is either blocking access to open copper sites of CuBTC, or it is interacting with the unsaturated copper sites themselves. Yet, under humid conditions, the CNCl loadings increase substantially as compared to the samples without TEDA. Certainly reactions are occurring, albeit slowly as seen by initial rapid breakthrough followed by slow elution to the feed concentration. Furthermore, the desorption curves indicate reactivity, as the effluent immediately returns to the baseline after feed termination. Overall, the CNCl loadings are slightly lower than the 3M broad spectrum carbon. Samples were also evaluated for their ability to remove ammonia and sulfur dioxide (Figures S2–S5 and Tables S2 and S3 in Supporting Information); ammonia results do indicate some degradation in performance due to the addition of TEDA, likely due to blockage of copper sites, and sulfur dioxide results also decrease slightly compared to the non-TEDA samples.

#### 4. CONCLUSIONS

Composite structures comprising varying percentages of zirconium hydroxide and the metal–organic framework CuBTC were evaluated as broad spectrum toxic chemical removal materials. A variety of characterization techniques such as XRD, ATR-FTIR, XPS, and SEM showed that the physical mixtures retained expected properties based on the weight percentages of the individual components. Even after pressing into pellets, the materials retained significant porosity and surface area.

Evaluation of the composites against ammonia showed increasing capacity with increasing CuBTC weight percent under both dry and humid conditions. In some cases, the composites exhibited synergistic effects, as the performance is greater than the weighted average of the two pure components. Sulfur dioxide, on the other hand, showed decreasing capacity with increasing CuBTC content, and no synergistic effects of mixing components. Cyanogen chloride capacity was substantial under dry conditions and composites exhibited

synergistic effects; however, almost no removal capabilities existed under humid conditions. The addition of TEDA to the materials resulted in slightly decreased CNCl removal under dry conditions, but significantly enhanced performance under humid conditions. In all, materials exhibited good broad spectrum removal capabilities. The ammonia performance of the composites were substantially higher than a broad spectrum carbon, while cyanogen chloride and sulfur dioxide removal capacities were slightly lower than those of the broad spectrum carbon.

## ■ ASSOCIATED CONTENT

### § Supporting Information

Full spectrum FTIR-ATR data, chemical removal capacities of a commercial broad spectrum material, and breakthrough curves for TEDA-impregnated samples. This material is available free of charge via the Internet at <http://pubs.acs.org>.

## ■ AUTHOR INFORMATION

### Corresponding Author

\*E-mail: gregory.w.peterson.civ@mail.mil. Tel.: (410) 436-9794. Fax: (410) 436-5513.

### Notes

The authors declare no competing financial interest.

## ■ ACKNOWLEDGMENTS

This work was completed under Defense Threat Reduction Agency (DTRA) Project BA07PRO104.

## ■ REFERENCES

- (1) Smith, J. W. H.; Westreich, P.; Croll, L. M.; Reynolds, J. H.; Dahn, J. R. Understanding the Role of Each Ingredient in a Basic Copper Carbonate Based Impregnation Recipe for Respirator Carbons. *J. Colloid Interface Sci.* **2009**, *337*, 313.
- (2) Petit, C.; Karwacki, C.; Peterson, G.; Bandosz, T. J. Interactions of Ammonia with the Surface of Microporous Carbon Impregnated with Transition Metal Chlorides. *J. Phys. Chem. C* **2007**, *111*, 12705.
- (3) Mahle, J. J.; Peterson, G. W.; Schindler, B. J.; Smith, P. B.; Rossin, J. A.; Wagner, G. W. Role of TEDA as an Activated Carbon Impregnant for the Removal of Cyanogen Chloride from Air Streams: Synergistic Effect with Cu(II). *J. Phys. Chem. C* **2010**, *114*, 20083.
- (4) Petit, C.; Peterson, G. W.; Mahle, J.; Bandosz, T. J. The Effect of Oxidation on the Surface Chemistry of Sulfur-Containing Carbons and their Arsine Adsorption Capacity. *Carbon* **2010**, *48*, 1779.
- (5) Seredych, M.; Mahle, J.; Peterson, G. W.; Bandosz, T. J. Interactions of Arsine with Nanoporous Carbons: Role of Heteroatoms in the Oxidation Process at Ambient Conditions. *J. Phys. Chem. C* **2010**, *114*, 6527.
- (6) Petit, C.; Levasseur, B.; Mendoza, B.; Bandosz, T. J. Reactive Adsorption of Acidic Gases on MOF/Graphite Oxide Composites. *Microporous Mesoporous Mater.* **2012**, *154*, 107.
- (7) Peterson, G. W.; Rossin, J. A.; Smith, P. B.; Wagner, G. W. Effects of Water on the Removal of Methyl Bromide Using Triethylene Diamine Impregnated Carbon. *Carbon* **2010**, *48*, 81.
- (8) TIC/TIM Task Force Memorandum for Record #1. TIC/TIM task Force Prioritization & Application Recommendations. Joint Program Executive Office for Chemical Biological Defense (JPEO-CBD), Office of the Secretary of Defense, United States Department of Defense, 2009.
- (9) Approval of Respiratory Protective Devices. *Code of Federal Regulations*, Part 84, Title 42, 1995.
- (10) Britt, D.; Tranchemontagne, D.; Yaghi, O. M. Metal–Organic Frameworks with High Capacity and Selectivity for Harmful Gases. *Proc. Natl. Acad. Sci. U.S.A.* **2008**, *105*, 11623.
- (11) Glover, T. G.; Peterson, G. W.; Schindler, B. J.; Britt, D.; Yaghi, O. MOF-74 building unit has a direct impact on toxic gas adsorption. *Chem. Eng. Sci.* **2011**, *66*, 163.
- (12) Chui, S. S.; Lo, S. M.; Charmant, J. P.; Orpen, A. G.; Williams, I. D. A Chemically Functionalizable Nanoporous Material [Cu<sub>3</sub>(TMA)<sub>2</sub>(H<sub>2</sub>O)<sub>3</sub>]<sub>n</sub>. *Science* **1999**, *283*, 1148.
- (13) Peterson, G. W.; Wagner, G. W.; Balboa, A.; Mahle, J.; Sewell, T.; Karwacki, C. J. Ammonia Vapor Removal by Cu<sub>3</sub>(BTC)<sub>2</sub> and Its Characterization by MAS NMR. *J. Phys. Chem. C* **2009**, *113*, 13906.
- (14) Decoste, J. B.; Peterson, G. W.; Smith, M. W.; Stone, C. A.; Willis, C. R. Enhanced Stability of Cu-BTC MOF via Perfluorohexane Plasma-Enhanced Chemical Vapor Deposition. *J. Am. Chem. Soc.* **2012**, *134*, 1486.
- (15) Peterson, G. W.; Wagner, G. W.; Keller, J. H.; Rossin, J. A. Enhanced Cyanogen Chloride Removal by the Reactive Zirconium Hydroxide Substrate. *Ind. Eng. Chem. Res.* **2010**, *49*, 11182.
- (16) Peterson, G. W.; Rossin, J. A. Removal of Chlorine Gases from Streams of Air Using Reactive Zirconium Hydroxide Based Filtration Media. *Ind. Eng. Chem. Res.* **2012**, *51*, 2675.
- (17) Peterson, G. W.; Karwacki, C. J.; Feaver, W. B.; Rossin, J. A. Zirconium Hydroxide as a Reactive Substrate for the Removal of Sulfur Dioxide. *Ind. Eng. Chem. Res.* **2009**, *48*, 1694.
- (18) Peterson, G. W.; Rossin, J. A.; Karwacki, C. J.; Glover, T. G. Surface Chemistry and Morphology of Zirconia Polymorphs and the Influence on Sulfur Dioxide Removal. *J. Phys. Chem. C* **2011**, *115*, 9644.
- (19) Bandosz, T. J.; Laskoski, M.; Mahle, J.; Mogilevsky, G.; Peterson, G. W.; Rossin, J. A.; Wagner, G. W. Reactions of VX, GD, and HD with Zr(OH)<sub>4</sub>: Near Instantaneous Decontamination of VX. *J. Phys. Chem. C* **2012**, *116*, 11606.
- (20) deKrafft, K. E.; Wang, C.; Lin, W. Metal–Organic Framework Templated Synthesis of Fe<sub>2</sub>O<sub>3</sub>/TiO<sub>2</sub> Nanocomposite for Hydrogen Production. *Adv. Mater.* **2012**, *24*, 2014–2018.
- (21) Jahan, M.; Bao, Q.; Loh, K. P. Electrocatalytically Active Graphene-Porphyrin MOF Composite for Oxygen Reduction Reaction. *J. Am. Chem. Soc.* **2012**, *134*, 6707–6713.
- (22) O'Neill, L. D.; Zhang, H.; Bradshaw, D. Macro-/Microporous MOF Composite Beads. *J. Mater. Chem.* **2010**, *20*, 5720–5726.
- (23) Petit, C.; Huang, L.; Jagiello, J.; Kenvin, J.; Gubbins, J.; Bandosz, T. J. *Langmuir* **2011**, *27*, 13043–13051.
- (24) Petit, C.; Bandosz, T. J. Exploring the Coordination Chemistry of MOF-Graphite Oxide Composites and their Applications as Adsorbents. *Dalton Trans.* **2012**, *41*, 4027.
- (25) Liu, X. M.; Rather, S.; Li, Q.; Lueking, A.; Zhao, Y.; Li, J. Hydrogenation of CuBTC Framework with the Introduction of a PtC Hydrogen Spillover Catalyst. *J. Phys. Chem. C* **2012**, *116*, 3477–3485.